

Aggregation Rate Measurements by Zero-Angle Time-Resolved Multiangle Laser Light Scattering

Ke Wang, Anup K. Singh, and John H. van Zanten*

Chemical Engineering Department, North Carolina State University,
Raleigh, North Carolina 27695-7905, and Chemical & Radiation Detection Laboratory,
Sandia National Laboratories, Livermore, California 94550

Received July 31, 2001. In Final Form: December 18, 2001

A new method for determining second-order aggregation rate constants via time-resolved multiangle laser light scattering is introduced. A major advantage of this approach is that second-order aggregation rate constants are determined without any assumptions regarding the dimer intraparticle interference or form factor. The second-order aggregation rate constants are calculated from the temporal variation of the zero-angle excess Rayleigh ratio within the context of von Smoluchowski's well-established model of colloidal aggregation. The new method is illustrated with two systems: (1) GM1-bearing liposomes aggregated in the presence of the cholera toxin B subunit and (2) sulfonated polystyrene latex aggregated in the presence of CaCl_2 . Whereas the method is demonstrated to be particularly well-suited for investigating slow aggregation processes, rapid aggregation processes are also accessible if proper precautions are taken.

Introduction

The stability and aggregation kinetics of liquid-dispersed colloidal particles lies at the heart of many technological processes including ceramic, magnetic, optical, and electrical material manufacturing; wastewater treatment; pharmaceutical formulation; and paint, coating and ink development. The kinetic stability of colloidal dispersions is of great significance to all colloid science. For instance, stability studies are often utilized in investigations of fundamental interparticle forces and hydrodynamic interactions. These stability studies are typically focused on investigations of aggregation or coagulation processes, particularly during their earliest stages, which facilitates the interpretation of the experimental measurements.

Colloidal aggregation phenomena have been studied by a wide variety of techniques. The most unambiguous methods involve direct counting via ultramicroscopy or particle counting.^{1–4} Unfortunately, these approaches are tedious and, as such, are not suitable for routine investigations of colloidal stability. Whereas turbidimetry provides a rapid means of qualitatively assessing aggregation phenomena,^{5,6} difficulties remain with quantitatively interpreting these measurements, although it should be noted that work is proceeding in this area.^{7,8} Additionally, static^{9,10} and dynamic^{11,12} light scattering methods are frequently used to monitor colloidal stability.

However, when considered individually, these previous light scattering methods require a priori knowledge of the dimer intraparticle interference or form factor, which is typically approximated by the Rayleigh–Gans–Debye method. This approximation was recently shown to be erroneous for sufficiently large scattering angles.¹³ Swiss researchers recently described a combined dynamic and static light scattering method that obviates the need for assuming an analytical form for the dimer form factor.¹⁴ One potential downfall of their proposed method is its economic viability, as it requires simultaneous dynamic and static light scattering measurements to be made at several angles, which is a potentially expensive undertaking if one considers the cost of purchasing multiple autocorrelators. Therefore, an alternative dimer-form-factor-independent method for determining second-order aggregation rate constants would be attractive.

In this paper, a new method for determining second-order aggregation rate constants from time-resolved multiangle laser light scattering is reported. The second-order aggregation rate constants are determined from the temporal variation of the excess Rayleigh ratio at zero scattering angle analyzed within the framework of von Smoluchowski's aggregation model. The primary advantage of this method is that it does not require a priori knowledge of the dimer intraparticle interference or form factor, unlike other individual light scattering methods. The method's utility is demonstrated with two completely different types of colloidal aggregation processes: (1) cholera toxin B subunit-induced aggregation of GM1-bearing liposomes and (2) CaCl_2 -induced aggregation of sulfonated polystyrene latex particles. The method is shown to be particularly useful for monitoring relatively slow aggregation processes.

Materials and Methods

Materials. Ganglioside GM1, L- α -distearoylphosphatidylcholine (DSPC), cholesterol, and cholera toxin B subunit were obtained from Sigma Chemical Co. (St. Louis, MO). Unilamellar liposomes with a composition of DSPC/cholesterol/GM1 in a 47.5:

* Corresponding author. E-mail: john_vz@ncsu.edu.

(1) Sonntag, H.; Strenge, K. *Coagulation Kinetics and Structure Formation*; Plenum Press: New York, 1987.

(2) Swift, D. L.; Friedlander, S. K. *J. Colloid Sci.* **1964**, *19*, 621.

(3) Matthews, B. A.; Rhodes, D. T. *J. Colloid Interface Sci.* **1970**, *32*, 332.

(4) Broide, M. L.; Cohen, R. J. *J. Colloid Interface Sci.* **1992**, *153*, 493.

(5) Ottewill, R. H.; Shaw, J. N. *Discuss. Faraday Soc.* **1966**, *42*, 154.

(6) Lichtenbelt, J. W. Th.; Pathmanathan, C.; Wiersema, J. J. *Colloid Interface Sci.* **1974**, *49*, 281.

(7) Maroto, J. A.; de las Nieves, F. J. *Colloid Polym. Sci.* **1997**, *275*, 1148.

(8) Maroto, J. A.; de las Nieves, F. J. *Colloids Surf. A* **1998**, *132*, 153.

(9) Lips, A.; Smart, C.; Willis, E. *J. Chem. Soc., Faraday Trans.* **1971**, *67*, 2979.

(10) van Zanten, J. H.; Elimelech, M. *J. Colloid Interface Sci.* **1992**, *154*, 1.

(11) Novich, B. E.; Ring, T. A. *Clays Clay Miner.* **1984**, *32*, 400.

(12) Virden, J. W.; Berg, J. C. *J. Colloid Interface Sci.* **1992**, *149*, 528.

(13) Holthoff, H.; Borkovec, M.; Schurtenberger, P. *Phys. Rev. E* **1997**, *56*, 6945.

(14) Holthoff, H.; Egelhaaf, S. U.; Borkovec, M.; Schurtenberger, P.; Sticher, H. *Langmuir* **1996**, *12*, 5541.

47.5:5 mole ratio were prepared by extrusion through polycarbonate membranes. Liposome preparation and characterization were performed as described previously.¹⁵ The extruded liposomes had a mean hydrodynamic diameter (determined by dynamic light scattering) of 125 nm and a zeta potential of -48.1 mV, and they contained approximately 10⁵ GM1 per liposome. Surfactant-free sulfate-functionalized 98 nm diameter polystyrene latex particles with a zeta potential of -60 mV were purchased from Interfacial Dynamics Corp. (Portland, OR) and used as received.

Time-Resolved Multiangle Laser Light Scattering. Time-resolved multiangle laser light scattering (TR-MALLS) measurements were performed with a DAWN DSP laser photometer (Wyatt Technology Inc., Santa Barbara, CA). Aggregation reactions were conducted in 20 mL glass scintillation vials, which were carefully cleaned, rinsed with filtered deionized water, and dried to eliminate any contaminants, including dust and ions. Before each experiment, samples were checked for clarity by measuring the solvent background scattering at very low angles and were discarded if the background noise was too high. Affinity liposome aggregation was initiated by adding cholera toxin B subunits to an existing affinity liposome solution to a final volume of 7 mL. In each case, to avoid bubble formation, the solution was gently mixed for approximately 2 s prior to measurements. Experiments were conducted at room temperature, approximately 23 °C, and repeated several times. Polystyrene latex particle aggregation reactions were performed in the same manner as described for the affinity liposome aggregation, with the particle aggregation being initiated by the addition of calcium chloride solution to a final volume of 5 mL.

The Rayleigh-Gans-Debye approximation was used to interpret the measured light scattering spectra. In principle, the method provides a measure of both the aggregate distribution weight-average molar mass and the z-average radius of gyration. The work described here requires only a measure of the excess Rayleigh ratio at zero scattering angle, as will be shown shortly. Because only very dilute solutions were considered, the influence of interparticle interactions on the measured weight-average molar mass was negligible. In the absence of interparticle interactions (i.e., sufficiently dilute solutions), the excess Rayleigh ratio is¹⁶

$$R_\theta = Kc\psi^2 M_w P_{LS}(q) \quad (1a)$$

where R_θ denotes the excess Rayleigh ratio, K is an optical constant, c is the mass concentration, ψ is the refractive index increment of the scatters, M_w is the aggregate weight-average molar mass, $P_{LS}(q)$ is the light scattering average intraparticle interference factor, and q is the scattered wavevector. The scattered wavevector is

$$q = \frac{4\pi n_s}{\lambda_o} \sin(\theta/2)$$

where n_s is the solvent refractive index, λ_o is the incident radiation wavelength in vacuo, and θ is the scattering angle. The weight-average aggregate molar mass is determined by extrapolating the measured angular variation of the excess Rayleigh ratios to zero scattering angle (i.e., $q = 0$), where $P_{LS}(q)$ becomes unity and the extrapolated value of R_θ is simply

$$R_{\theta=0} = K'c\psi^2 M_w \quad (1b)$$

The extrapolation of the measured excess Rayleigh ratios to zero angle is done via a second-order expansion of the intraparticle interference factor

$$R_\theta \approx K'c\psi^2 M_w \left(1 - \frac{q^2 \langle R_g^2 \rangle_z}{3} + \alpha q^4 \right) \quad (1c)$$

where R_g is the radius of gyration, z denotes a z -averaged quantity, and α is a constant that contains higher-order size information.

The extrapolation procedure is very effective for two reasons. First, only relatively small primary particles are considered (i.e., diameters ≈ 100 nm). Second, only the earliest stages of aggregation are considered. In fact, data analysis is limited to the time range for which the zero-angle excess Rayleigh ratio increases by a factor of 1.25 or less. These two conditions ensure that the second-order component of the extrapolation (i.e., the q^4 term) is a very small correction to the usual $R_\theta \sim q^2$ approximation. It should be noted that the same approach has been used with great success to investigate DNA condensation with cationic polymers, where the zero-angle excess Rayleigh ratio increases by a factor of nearly 1000.¹⁷ The approach can be easily extended to larger particles if sufficiently small scattering angles are accessible to facilitate the extrapolation process.

Zero-Angle Light Scattering from an Aggregating Colloidal Suspension

Time-resolved multiangle laser light scattering provides a means for determining the temporal evolution of the weight-average molar mass of an aggregating colloidal suspension. To interpret such measurements, it is necessary to formulate a kinetic model of the aggregation process. Such a model was originally developed by von Smoluchowski, whose theory of colloidal aggregation yields the following expression for the number of m -mer aggregates, $N_m(t)$ ¹⁸

$$N_m(t) = N_0 \frac{\tau^{m-1}}{(1 + \tau)^{m+1}} \quad (2)$$

In eq 2, N_0 is the initial number of unaggregated colloidal particles, and the dimensionless aggregation time τ is given by $\tau = kN_0 t$, where k is a second-order aggregation rate constant and t denotes the actual aggregation or reaction time. Under Brownian diffusion control, the maximum or rapid second-order aggregation rate constant is simply $k_R = 4k_B T/3\eta$, where k_B is the Boltzmann constant, T is the solution temperature, and η is the solvent viscosity.¹⁸ Deviations from this rapid second-order aggregation rate constant occur in the presence of colloidal forces¹⁹ (e.g., electrostatic, hydration, steric, etc.) or hydrodynamic interactions^{19,20} or, in the case of colloidal aggregation driven by specific interactions, as a result of the number of accessible binding sites. These factors can be accounted for via a collision efficiency α_p such that $k = \alpha_p k_R$. It should be noted that the von Smoluchowski model assumes that collisions between aggregates of approximately equal sizes dominate the aggregation process and that the collision efficiency is independent of aggregate size. This simple model has been found to describe rapid aggregation processes very accurately,²¹ although deviations are observed for slow aggregation at long times ($\alpha_p \ll 1$).²² The method described here utilizes sufficiently short aggregation times to enhance the applicability of the von Smoluchowski colloidal aggregation theory.²³

As noted previously, multiangle laser light scattering measurements provide a means for determining the weight-average molar mass of an aggregate dispersion.

(17) Lai, E.; van Zanten, J. H. *Biophys J.* **2001**, *80*, 864.

(18) von Smoluchowski, M. *Z. Phys. Chem.* **1917**, *92*, 129.

(19) Russel, W. B.; Saville, D. A.; Schowalter, W. R. *Colloidal Dispersions*; Cambridge University Press: New York, 1989.

(20) Shilov, V.; Lichtenfeld, H.; Sonntag, H. *Colloids Surf. A* **1995**, *104*, 321.

(21) Higashitani, K.; Matsuno, Y. *J. Chem. Eng. Jpn.* **1979**, *12*, 460.

(22) Weitz, D. A.; Lin, M. Y.; Huang, J. S. In *Complex and Supramolecular Fluids*; Safran, S. A., Clark, N. A., Eds.; Wiley-Interscience: New York, 1986; p 509.

(23) Holthoff, H.; Schmitt, A.; Fernández-Barbaro, A.; Bortovec, M.; Cabrerizo-Vilchez, M. A.; Schurtenberger, P.; Hidalgo-Álvarez, R. *J. Colloid Interface Sci.* **1997**, *192*, 463.

(15) Singh, A. K.; Harrison, S. H.; Schoeniger, J. S. *Anal. Chem.* **2000**, *72*, 6019–6024.

(16) Zimm, B. H. *J. Chem. Phys.* **1948**, *16*, 1093.

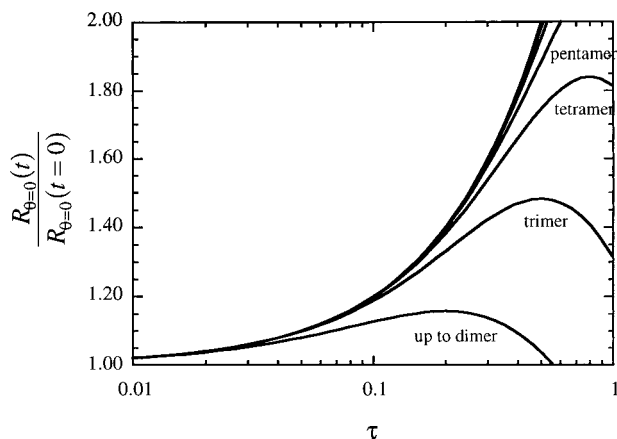


Figure 1. Temporal variation of the predicted normalized zero-angle excess Rayleigh ratio as calculated from eq 4 in the text. The curves correspond to an ever-increasing number of terms retained in the expression ranging from two to nine. It is readily apparent that for normalized Rayleigh ratios of 1.25, the retention of aggregates up to and including pentamers provides a very accurate approximation of the aggregation process.

An aggregate weight-average molar mass is computed from the von Smoluchowski aggregation model in a straightforward manner using

$$M_w(t) = \frac{M_1^2 \sum_{m=1}^{\infty} m^2 N_m(t)}{N_0 M_1} = M_1 \sum_{m=1}^{\infty} m^2 \frac{\tau^{m-1}}{(1+\tau)^{m+1}} \quad (3)$$

Here, M_1 denotes the molar mass of an unaggregated primary particle. Given this expression for the time-dependent aggregate weight-average molar mass, the second-order aggregation rate constant, k , is readily determined from the temporal variation of the normalized zero-angle excess Rayleigh ratio, as

$$\frac{R_{\theta=0}(t)}{R_{\theta=0}(t=0)} = \frac{M_w(t)}{M_1} = \sum_{m=1}^{\infty} m^2 \frac{\tau^{m-1}}{(1+\tau)^{m+1}} = \sum_{m=1}^{\infty} m^2 \frac{(kN_0 t)^{m-1}}{(1+kN_0 t)^{m+1}} \quad (4)$$

This expression is based on the assumption that the refractive index increment of the aggregates is the same as that of the unaggregated primary particles or monomers. Once again, it should be noted that interaggregate interactions are assumed to be negligible here. This formulation provides a framework for determining second-order aggregation rate constants even in the absence of particle optical properties as it only requires determination of the temporal variation of the zero-angle excess Rayleigh ratio. The normalized zero-angle excess Rayleigh ratio temporal variation predicted by eq 4 is shown in Figure 1. Although the predicted result is very sensitive to the number of terms retained in eq 4, as expected, it is apparent that, for sufficiently small values of τ , the expression can be truncated at a fairly small number of terms with very little loss of accuracy.

The zero-angle excess Rayleigh ratio is easily measured with time-resolved multiangle light scattering provided that two conditions are met to ensure accurate extrapolation to zero scattering angle. First, sufficiently small primary particles must be considered to minimize the

angular variation of the intraparticle interference or form factors, thereby facilitating the extrapolation to zero angle. Second, only aggregation processes that are slow enough to allow for collection of statistically significant data prior to the formation of large aggregates should be considered. It should be noted that the latter condition is readily moderated via the initial monomer concentration. The measurements reported here have been restricted to times where

$$\frac{R_{\theta=0}(t)}{R_{\theta=0}(t=0)} \leq 1.25$$

As is readily apparent in Figure 1, this provides an upper bound for the dimensionless aggregation time, $\tau = 0.125$. This value of τ is significantly shorter than the particle half-life, $\tau_{1/2} = 1$, where the particle half-life is defined to be the time at which the total number particles (unaggregated monomers plus aggregates) is one-half of the number of initial primary particles. It should be noted that the upper bound on the dimensionless time is also several times smaller than the time at which the free monomer concentration has been reduced to one-half its original value, $\tau = 2^{1/2} - 1$. It can also be observed in Figure 1 that this restriction allows the normalized weight-average molar mass temporal evolution expression, eq 4, to be truncated after only five terms (i.e., aggregates up to pentamer size) without any significant resulting error. Most importantly, this general rule also ensures that only the earliest stage of the aggregation process is considered, and therefore, it allows for the study of both rapid and slow aggregation processes, as deviations from the von Smoluchowski theory have been observed for the latter at sufficiently long times.

Results and Discussion

Gangliosides are natural receptors for a number of bacterial toxins and viruses.¹⁵ Because the cholera toxin B subunit binds ganglioside GM1 very specifically and multivalently,²⁴ GM1-bearing liposomes will aggregate following the introduction of cholera toxin B subunit to solution. Cholera toxin B subunit is a pentamer and can bind up to five GM1 molecules simultaneously. Recently, specific interaction-controlled colloidal assembly has been proposed as a potential method for building complex nanostructures.^{25,26} Our primary interests lie in developing affinity-liposome-based methods for detecting bacterial and viral toxins and methods for removing these toxins from water.¹⁵ The temporal evolution of the normalized zero-angle excess Rayleigh ratios for the same dispersion concentration of GM1-bearing liposomes ($N_0 = 1.7 \times 10^{10} \text{ cm}^{-3}$) aggregating in the presence of cholera toxin B subunit at different concentrations is shown in Figure 2. Owing to the very large liposome molar masses considered here, the scattering contribution of any free cholera toxin B subunit can be neglected. The strong binding between cholera toxin B subunits and ganglioside GM1 sites on the liposomes drives the aggregation, as each cholera toxin B subunit can accommodate 5 GM1 gangliosides. Because the lowest cholera toxin B subunit concentration considered corresponds to an affinity liposome/cholera toxin B subunit mole ratio of nearly 1:500, it is most likely that the earliest stages of the aggregation process will not be

(24) van Heyningen, W. E. *Nature* **1974**, *249*, 415–417.

(25) Kisak, E. T.; Kennedy, M. T.; Trommeshauser, D.; Zasadzinski, J. A. *Langmuir* **2000**, *16*, 2825.

(26) Walker, S. A.; Kennedy, M. T.; Zasadzinski, J. A. *Nature* **1997**, *387*, 61.

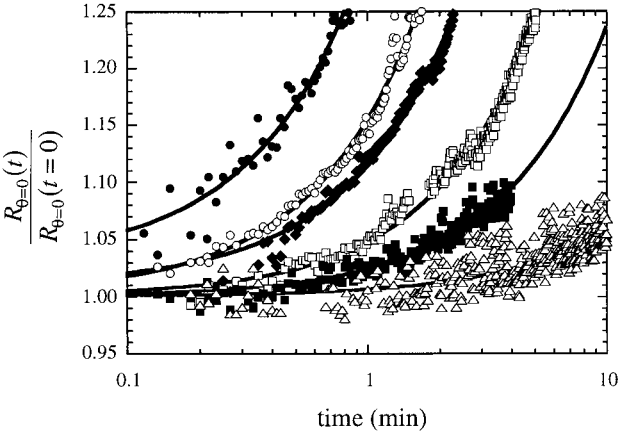


Figure 2. Temporal variation of the normalized zero-angle excess Rayleigh ratio of GM1-bearing liposomes aggregating in the presence of cholera toxin B subunit at pH 4.8. The fitted curves represent the von Smoluchowski theory of colloidal aggregation up to and including pentamers. The initial GM1-bearing liposome concentration is $1.7 \times 10^{10} \text{ cm}^{-3}$. The cholera toxin B subunit concentrations are as follows: (●) 2.10×10^{-5} , (○) 1.57×10^{-5} , (◆) 1.26×10^{-5} , (□) 1.05×10^{-5} , (■) 6.29×10^{-6} , and (△) $2.07 \times 10^{-6} \text{ mM}$. The second-order aggregation rate constants are tabulated in Table 1.

affected by the finite cholera toxin B concentration and that the von Smoluchowski model should be applicable. The fitted curves in Figure 2 are the normalized zero-angle excess Rayleigh ratio temporal variations predicted from the von Smoluchowski aggregation theory (eq 4) fitted to the experimental data where aggregates up to and including pentamers are considered. The only adjustable parameter in these fits is the second-order aggregation rate constant, k . It is apparent that the agreement between the model prediction and experimental data is very good.

As noted previously, the ultimate extent of aggregation is limited by the cholera toxin B subunit/ganglioside GM1 mole ratio and the amount of ganglioside GM1 present in the affinity liposomes, and only the very earliest times were considered in the model fit to ensure that the initial second-order aggregation rate constant was essentially unchanging. This is important, as the reaction kernels will ultimately be time-dependent because the aggregation process is driven by cholera toxin B subunit-GM1 specific interactions.²³ As shown in Figure 2, the aggregation rate increases as expected with increasing cholera toxin B subunit concentration. As further confirmation of the success of the von Smoluchowski model and the success of the zero-angle excess Rayleigh ratio approach for investigating colloidal aggregation, the results of Figure 2 are scaled onto a master curve in Figure 3, where the x axis is the dimensionless aggregation time τ . It is apparent that the proposed model describes the experimental measurements very well.

The second-order aggregation rate constants for the affinity liposome aggregation assays shown in Figure 1 are tabulated in Table 1, along with those found for several other cholera toxin B subunit concentrations. Because the upper Brownian diffusion bound on the second-order aggregation constant is $\sim 6 \times 10^{-12} \text{ cm}^3/\text{s}$, the second-order aggregation rate constants are rather small at the lower cholera toxin B subunit concentrations. This results directly from the limited number of active binding or aggregation sites. For example, at the lowest toxin concentration considered, the cholera toxin B subunit/GM1 mole ratio is 6.9×10^{-4} , and k is $2.85 \times 10^{-15} \text{ cm}^3/\text{s}$, whereas at the highest cholera toxin B subunit concentration considered, the cholera toxin B subunit/GM1 mole

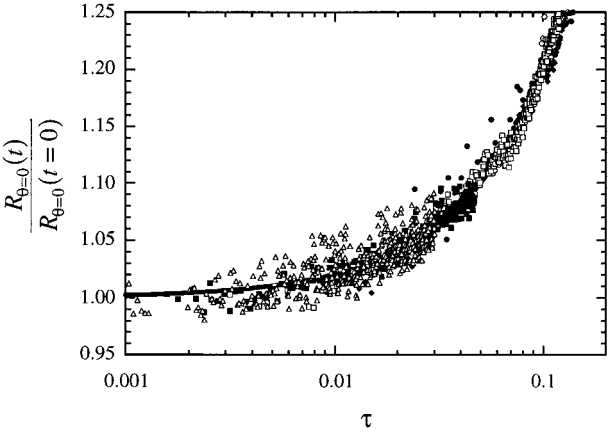


Figure 3. Reduced time dependence of the normalized zero-angle excess Rayleigh ratio of GM1-bearing liposomes aggregating in the presence of cholera toxin B subunit at pH 4.8. The initial GM1-bearing liposome concentration is $1.7 \times 10^{10} \text{ cm}^{-3}$. The symbols are the same as in Figure 2.

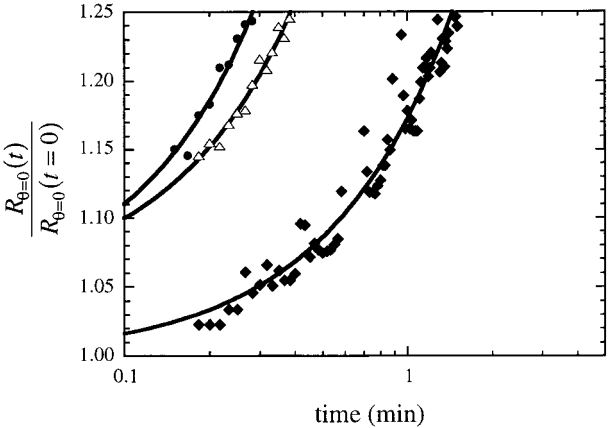


Figure 4. Temporal variation of the normalized zero-angle excess Rayleigh ratio of 98 nm diameter sulfonated polystyrene particles aggregating in the presence of CaCl_2 at pH 5.7. The curves represent the von Smoluchowski theory of colloidal aggregation fitted to experimental data (see text). The initial lattice concentration is $5.1 \times 10^{10} \text{ cm}^{-3}$. The CaCl_2 concentrations are as follows: (◆) 5, (△) 10, and (●) 15 mM. The measured second-order aggregation rate constants are listed in Table 1.

Table 1. Summary of Second-Order Aggregation Rate Constants

GM1-bearing liposomes $N_0 = 1.7 \times 10^{10} \text{ cm}^{-3}$		sulfonated polystyrene lattices $N_0 = 5.1 \times 10^{10} \text{ cm}^{-3}$	
[cholera toxin B] ^a (mM)	k (cm^3/s)	[CaCl_2] (mM)	k (cm^3/s)
2.07×10^{-6}	2.85×10^{-15}	5	1.70×10^{-12}
6.29×10^{-6}	1.13×10^{-14}	10	4.88×10^{-12}
1.05×10^{-5}	2.28×10^{-14}	15	7.14×10^{-12}
1.26×10^{-5}	5.40×10^{-14}		
1.41×10^{-5}	8.15×10^{-14}		
2.10×10^{-5}	1.55×10^{-13}		
2.55×10^{-5}	4.16×10^{-13}		
3.82×10^{-5}	7.20×10^{-13}		
7.26×10^{-5}	1.43×10^{-12}		

^a This is the concentration of cholera toxin B subunits.

ratio is 2.42×10^{-2} , and k is $1.43 \times 10^{-12} \text{ cm}^3/\text{s}$. It is clear not only that cholera toxin B subunit induces aggregation, but also that the cholera toxin B subunit/GM1 mole ratio determines the aggregation rate, as expected. It should be noted that the aggregation rate also depends on the overall concentration of GM1 in the systems.²⁷

As an illustration of the potential difficulty of monitoring rapid aggregation processes with this technique, data are

shown for CaCl_2 -induced aggregation of sulfonated polystyrene particles in Figure 3 ($N_0 = 5.1 \times 10^{10} \text{ cm}^{-3}$). Once again, in all cases, the agreement between the model predictions and experimental data is excellent. Second-order aggregation rate constants were found to increase with increasing salt concentration. However, for the two most rapid aggregation assays (10 and 15 mM CaCl_2), the measured rate constants are larger than expected, with the 15 mM case actually being larger than the theoretical upper bound! This is an example of when the proposed approach can fail because aggregation under these conditions is too rapid to assess with the zero-angle excess Rayleigh ratio method. The “good” agreement between theory and experiment is because the errors in the aggregation initiation time and mixing time are of nearly the same order as the observation time. That is, the agreement is purely fortuitous in this case. Therefore, another good general rule is that only aggregation processes for which the zero-angle excess Rayleigh ratio increases by only a few percent for $\tau = 0.1$ should be considered. Whereas one possible solution to this dilemma is to reduce the aggregation rate by simply reducing the initial particle concentration, it should be noted that the initial particle concentration can only be reduced insofar that the initial particle dispersion still displays sufficient scattering power. The measured second-order aggregation rate constant found for the 5 mM CaCl_2 solution is within a factor of 2 of previous values found for PS latex particles of nearly the same surface chemistry.^{10,13,14,21,28,29} This is satisfactory agreement, especially in light of previous observations of the extreme sensitivity of the second-order aggregation rate constant to trace impurities.¹⁴

(27) Wang, K.; Singh, A. K.; van Zanten, J. H. Manuscript in preparation.

Conclusion

A new method for determining second-order aggregation rate constants via time-resolved multiangle laser light scattering was developed. A major advantage of this approach is that second-order aggregation rate constants can be determined without any assumptions regarding the dimer intraparticle interference or form factor. The second-order aggregation rate constants were calculated from the temporal variation of the zero-angle excess Rayleigh ratio within the context of von Smoluchowski's well-established model of colloidal aggregation. The criteria for applying the new approach were described in detail. The method was illustrated with two systems: (1) GM1-bearing liposomes aggregated in the presence of cholera toxin B subunit and (2) sulfonated polystyrene latex aggregated in the presence of CaCl_2 . Whereas the method was demonstrated to be particularly well-suited for investigating slow aggregation processes, it was shown that rapid aggregation processes can also be studied if proper precautions are taken.

Acknowledgment. The authors thank Mr. Daniel Throckmorton for his assistance in preparing the GM1-bearing liposomes and Mr. James D. Arroway for critically reading the manuscript. K.W. and J.H.v.Z. also acknowledge the support of the National Science Foundation via Grant CTS-9702413.

LA0112070

(28) Behrens, S. H.; Borkovec, M.; Schurtenberger P. *Langmuir* **1998**, *14*, 1951.

(29) Behrens, S. H.; Christl, D. I.; Emmerzael, R.; Schurtenberger, P.; Borkovec, M. *Langmuir* **2000**, *16*, 2566.